

INTRODUCTION

The Greenwood Lake and Sloatsburg quadrangles, in northern New Jersey in Sussex, Passaic and Bergen Counties, are situated in the northeastern part of the New Jersey Highlands Physiographic Province. The Wanauke River is the primary drainage in the map area and its impoundment created the Monksville Reservoir, a northern extension of the Wanauke Reservoir system. The topography of the map area is characterized by rugged uplands that include large tracts of land currently undeveloped and managed by the North Jersey District Water Supply Commission, or by the New Jersey Department of Environmental Protection's State Parks and Wildlife Management Area lands. East of Greenwood Lake, the topography is dominated by ridges and stream valleys of varied orientation that reflect the structural complexity and non-linear trend of the underlying Mesoproterozoic bedrock. West of Greenwood Lake, and extending to the area of Upper Greenwood Lake, the topography is more linear due to the relatively uniform trend of the underlying Paleozoic bedrock. Northwest of the Paleozoic bedrock, the topography is more varied because of the more linear trend of the underlying Mesoproterozoic bedrock.

This report provides detailed geologic information on the stratigraphy, structure and description of geologic units in the map area. Cross-section A-A' shows a vertical profile of the geologic units and their structure. Rose diagrams in figures 1-4 provide a directional analysis of selected structural features. The interpretations presented here supersede those shown on previous bedrock geologic maps of the area.

STRATIGRAPHY
Paleozoic Rocks

The youngest bedrock in the map area is Silurian and Devonian that crops out on, and along, Bearfoot Mountain, in the Green Pond Mountain Region, a northeast-trending block of downlifted and folded Paleozoic sedimentary rocks that extends through the western part of the area. The Paleozoic formations include the Green Pond Conglomerate, Longwood Shale, Pocono Island, and Berkshire Valley Formations of Silurian-age, and the Connelly Conglomerate, Esopus Formation, Kanouse Sandstone, Cornwall Shale, Bellevue Sandstone and Skunnumuk Conglomerate of Devonian-age. The origin and stratigraphic relationships of these formations is discussed by Darton (1894), Kimmel and Waller (1950), Barnett (1970, 1976), and Herman and Mitchell (1991).

Mesoproterozoic Rocks

A single diabase dike about 25 feet wide intrudes Mesoproterozoic rocks along the north shore of Monksville Reservoir, at the southern edge of the Greenwood Lake quadrangle. Its strike length is unknown because it cannot be traced to the north due to the lack of exposure, or to the south because it is beneath the reservoir. The dike strikes nearly due north and dips steeply east. It has sharp contacts and chilled margins against enclosing Mesoproterozoic rocks. The dike correlates spatially and temporally to similar dikes in the Highlands that are interpreted as having been emplaced into a rift-related, extensional tectonic setting at about 600 Ma during breakup of the supercontinent Rodinia (Volkert and Puffer, 1995).

Mesoproterozoic Rocks

Most of the map area is underlain by rocks of Mesoproterozoic age. These include an assemblage of various granites and gneisses, most of which were metamorphosed to granulite facies during the Ottawa phase of the Grenville orogeny at 1045 to 1024 Ma (Volkert and others, 2010). The temperature for this high-grade metamorphism averages 750°C based on a regional study using calcite-granite geothermometry (Peck and others, 2006).

The oldest Mesoproterozoic rocks are the Losee Suite (Drake, 1984; Volkert and Drake, 1999) and a ductile assemblage of supracrustal metasedimentary and metasedimentary rocks (Volkert, 2004). Calcic rocks of the Losee Suite include various quartz-rich gneisses mapped as quartz-oligoclase gneiss, biotite-quartz-oligoclase gneiss, hornblende-quartz-plagioclase gneiss, and hypersthene-quartz-plagioclase gneiss; and quartz-poor rock mapped as diorite, and amphibole formed in a magmatic arc tectonic setting (Volkert, 2004). The Losee Suite yielded sensitive high-resolution ion microprobe (SHRIMP) U-Pb zircon ages of 1282 to 1248 Ma (Volkert and others, 2010). Spatially and temporally associated with the Losee Suite are supracrustal rocks that include potassic leucogranite gneiss and amphibolite all of which formed from felsic and mafic volcanic protoliths, respectively, and quartzfeldspathic gneisses and calcic rocks formed from sedimentary protoliths. Supracrustal rocks were deposited in a back-arc basin situated inland of the Losee arc (Volkert, 2004). Supracrustal volcanic rocks yielded U-Pb SHRIMP zircon ages of 1299 to 1251 Ma (Volkert and others, 2010) that closely overlap the ages of the Losee Suite. Amphibolite associated with the Losee Suite is metaclastic, whereas amphibolite associated with the supracrustal gneisses may be metaclastic or metasedimentary in origin. All variants of amphibolite are undifferentiated on the map.

Hornblende-bearing granite and related rocks of the Byram Intrusive Suite, that comprise part of the Vernon Supersuite (Volkert and Drake, 1996), are abundantly exposed in the map area where they intrude Losee Suite and supracrustal rocks. Byram rocks form a complete differentiation series that includes quartz monzonite, granite, and alkalsite, all of which have a distinctive A-type geochemical composition (Volkert and others, 2000). Byram granite in the Newfoundland quadrangle south of the map area, and elsewhere in the western Highlands, yielded U-Pb SHRIMP zircon ages of 1185 to 1182 Ma (Volkert and others, 2010).

The youngest Mesoproterozoic rocks are potassic-granite pegmatites that are undeformed, contain xenoliths of foliated gneiss, and intrude other Mesoproterozoic rocks in the area as small, tabular to irregular bodies that are discordant to metamorphic foliation. They form bodies too small to be shown on the map. Pegmatites yielded zircon U-Pb ages of 960 to 965 Ma (Volkert and others, 2005).

STRUCTURE
Paleozoic Bedding

Bedding in the Paleozoic formations of the Green Pond Mountain Region is fairly uniform and strikes at an average of N 38° E. Beds are predominantly overturned and dip steeply southeast and, less commonly, northwest. They range in dip from 5° to 90° and average 70°.

Mesoproterozoic Foliation

Crystallization foliation, formed by the parallel alignment of mineral grains in the Mesoproterozoic rocks, defines the trend of the bedrock. It is an inherited feature from compressional stresses during granulite-facies metamorphism that deformed the rocks between 1045 and 1024 Ma (Volkert and others, 2010). Foliations are variably in the strike because of deformation of the rocks during folding, but they are somewhat more uniform in the western part of the area where they strike mainly northeast. Foliations in the Greenwood Lake quadrangle strike N 28° E, on average (fig. 1) and N 33° E, in the Sloatsburg quadrangle (fig. 2). Foliations dip mainly southeast and, very locally, northwest except in the fringe areas of folds where they dip north. The dip of all foliations ranges from 7° to 90° and averages 55°.

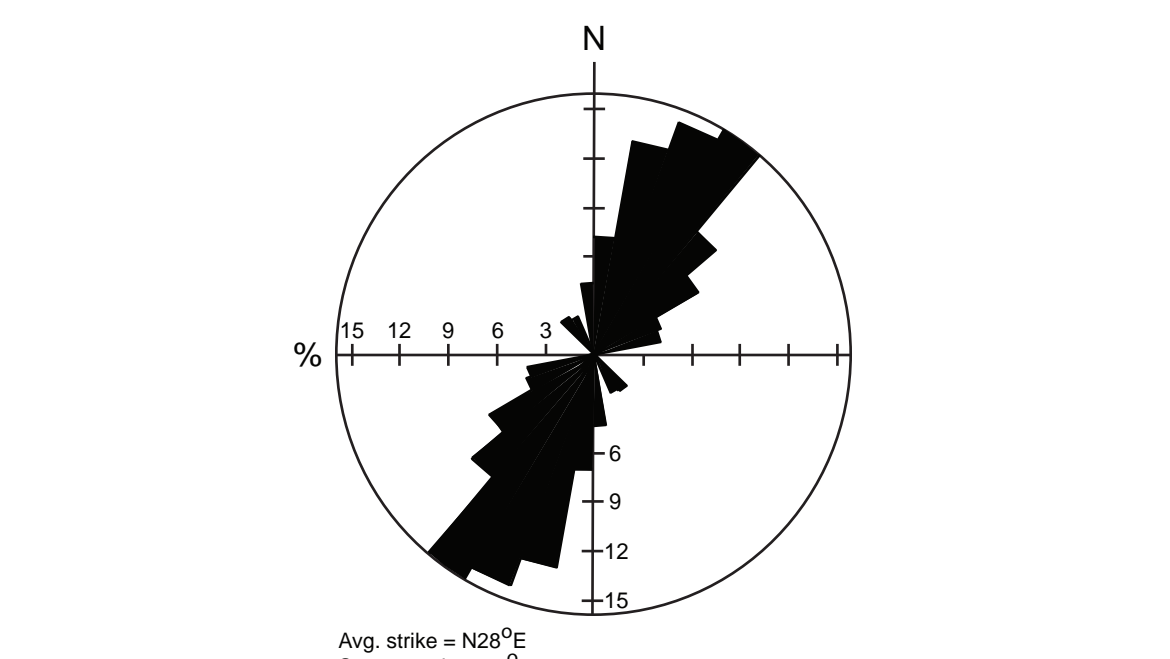


Figure 1. Rose diagram of the strike of crystallization foliations in Mesoproterozoic rocks of the Greenwood Lake quadrangle.

Folds

Folds in the Paleozoic rocks are dominated by a southwest-plunging northwest-overturned syncline on Bearfoot Mountain (Herman and Mitchell, 1991), the axis of which extends along the ridge crest in the Skunnumuk Conglomerate. Both limbs of the fold dip steeply southeast.

Folds that deform Mesoproterozoic rocks originated during the Ottawa phase of the Grenville orogeny. They deform earlier-formal planar metamorphic fabrics and, therefore, postdate the development of crystallization foliation. Characteristic fold styles in the Mesoproterozoic rocks display three principal geometries. The earliest recognized fold phase consists of east-northeast-plunging, upright to northwest-overturned or southeast-overturned antiforms and synforms. These folds are refolded by the more regionally pervasive northeast-plunging, northwest-overturned antiforms and synforms that have north-trending axial surfaces. The axial surfaces of both fold phases are refolded by a third fold phase that consists of northeast-plunging, northwest-overturned antiforms and synforms that have northeast-trending axial surfaces. The overall sequence of folding is interpreted to represent changing vectors of compressive stress that were roughly synchronous with the granulite facies metamorphism. The plunge of all mineral lineations ranges from 5° to 58° (averaging 30°) to N 77° E, to N 76° E, with most lineations plunging N 45° E. No lineations or folds plunging southwest were recognized in Mesoproterozoic rocks.

Faults

Northeast-trending faults are common in this map area and they deform Mesoproterozoic and Paleozoic rocks. They include the Reservoir, Union Valley, Greenwood Lake, Green Turtle Pond, Wanauke River, and Ringwood Faults. Deformation includes ductile and brittle fabrics. Brittle deformation fabric consists of breccia, gouge, retrogression of mafic mineral phases, chlorite or epidote-coated fractures or slickensides, and (or) close-spaced fracture cleavage. Ductile deformation fabric consists of mylonite, boudinage and shear folds.

The Reservoir Fault strikes about N 40° E and varies in dip from steeply northwest to steeply southeast. It places Paleozoic rocks on the hanging wall against Mesoproterozoic rocks on the footwall along most of its length. The fault has undergone multiple reactivations during from the Proterozoic that include normal, right-lateral strike-slip, and reverse movement, but latest movement was reverse (Herman and Mitchell, 1991). The fault is characterized by a zone of brittle fabric of unknown width. The Green Pond Lake Fault places Paleozoic rocks on the footwall against Mesoproterozoic rocks on the hanging wall. It strikes N 40° E, and dips southeast at about 60°, either merging with, or cut by the Union Valley Fault in the subsurface. The latest movement was reverse (Herman and Mitchell, 1991). The fault is characterized by a zone of brittle fabric of unknown width.

The Union Valley Fault and Greenwood Lake Fault were mapped by Herman and Mitchell (1991) on the basis of missing stratigraphic units along strike to the south. Both faults extend along the northwest side of Greenwood Lake. The Union Valley Fault is bounded by Paleozoic rocks on both sides. It strikes N 40° E on average, and dips southeast at about 50°. The latest movement was reverse (Herman and Mitchell, 1991). The fault is characterized by a zone of brittle fabric of unknown width. The Greenwood Lake Fault places Paleozoic rocks on the footwall against Mesoproterozoic rocks on the hanging wall. It strikes N 40° E, and dips southeast at about 60°, either merging with, or cut by the Union Valley Fault in the subsurface. The latest movement was reverse (Herman and Mitchell, 1991). The fault is characterized by a zone of brittle fabric of unknown width.

The Green Turtle Pond Fault was identified in the Greenwood Lake quadrangle by the author during the rehabilitation of the dam at the south end of Green Turtle Pond (now known as Lake Awosting). It has also been recognized along strike to the south in the Wanauke (Volkert, 2011) and Newfoundland quadrangles (Volkert and others, 2010). The fault strikes northeast and dips northwest at about 70°. It is cut off on the north by the newly named Wanauke River Fault, and to the south it continues into the Newfoundland quadrangle where it may continue beneath the unconformity in Silurian rocks on Kanouse Mountain. The fault separates Mesoproterozoic rocks on both sides. Latest movement was dip-slip reverse. The fault is characterized by brittle deformation fabric that is about 100 feet wide.

The Wanauke River Fault was first identified by Hotz (1952) and its strike length was doubled during the current mapping. Although not well exposed, except in outcrops along the Wanauke River in the Wanauke Wildlife Management Area, the fault forms a well-defined lineament on aerial photographs. To the east it continues into Orange County, New York, and to the west it is cut off by the Greenwood Lake Fault. The Wanauke River Fault strikes N 70° E, and dips north at about 80°. It records dip-slip normal movement but also preserves evidence for right-lateral strike-slip movement. It is bounded by Mesoproterozoic rocks on both sides. The fault is characterized by a zone of brittle deformation fabric as much as 200 feet wide.

The newly named Ringwood Fault in the southeastern part of the quadrangle strikes N 45° E, and dips southeast at about 80°. It continues north into Orange County, New York, and south into the Wanauke quadrangle, although it was not recognized there prior to publication of this map (Volkert, 2011). The fault is bounded by Mesoproterozoic rocks on both sides. It is characterized by brittle deformation fabric about 100 feet wide.

Joints

Joints are a ubiquitous feature in the Paleozoic and Mesoproterozoic rocks but are best developed in massive rocks such as Paleozoic sandstones, quartzite and conglomerate, and in Mesoproterozoic granite and some gneiss. Joints are characteristically planar, moderately well formed, and moderately to steeply dipping. They vary in spacing from a foot to tens of feet apart. Their surfaces are typically unmineralized, except near faults, and are smooth and, less commonly, slightly irregular.

In the Paleozoic rocks, northeast-trending cross joints are the most common. They dip moderately to steeply and nearly equally to the northeast or southwest (Herman and Mitchell, 1991). The dominant joints in Mesoproterozoic rocks are nearly perpendicular to the strike of crystallization, a consistent feature in Mesoproterozoic rocks throughout the Highlands (Volkert, 1996). Therefore, their strike is somewhat varied because of folding. The dominant joints in Mesoproterozoic rocks of the Greenwood Lake quadrangle strike N 52° W, on average (fig. 3) and dip mainly southwest. A subordinate set strikes about N 20° E, and dips nearly equally northwest or southeast. The dip of both sets ranges from 50° to 90° and averages 72°. The dominant joints in the Sloatsburg quadrangle strike N 62° W, on average (fig. 4) and dip mainly southwest. A subordinate set strikes N 35° E. The dip of both sets ranges from 25° to 90° and averages 67°.

ECONOMIC RESOURCES

Mesoproterozoic rocks in the map area, and particularly those in the Losee Suite, host economic deposits of iron ore (magnetite) that was mined predominantly during the 19th century. Iron mines are widespread throughout the area, but the largest and most important ones are in the southeastern part, in the Ringwood district. Detailed descriptions of most of the mines are given in Bayley (1910), Hotz (1952), and unpublished abandoned mines database of the New Jersey Geological and Water Survey. Exploration for uranium took place during the middle of the 20th century in the northwestern part of the map area, north of Upper Greenwood Lake, on some promising aeroradiometric anomalies, but mining leases never were acquired so no mining occurred. Mesoproterozoic rocks east and south of Greenwood Lake were quarried for crushed stone.

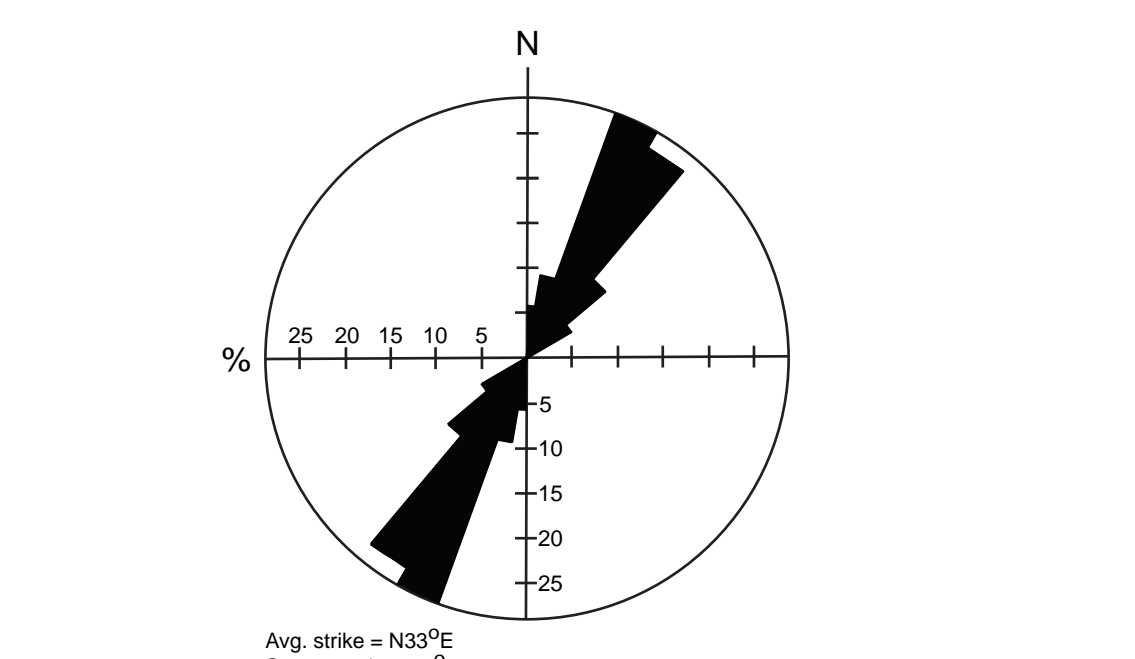
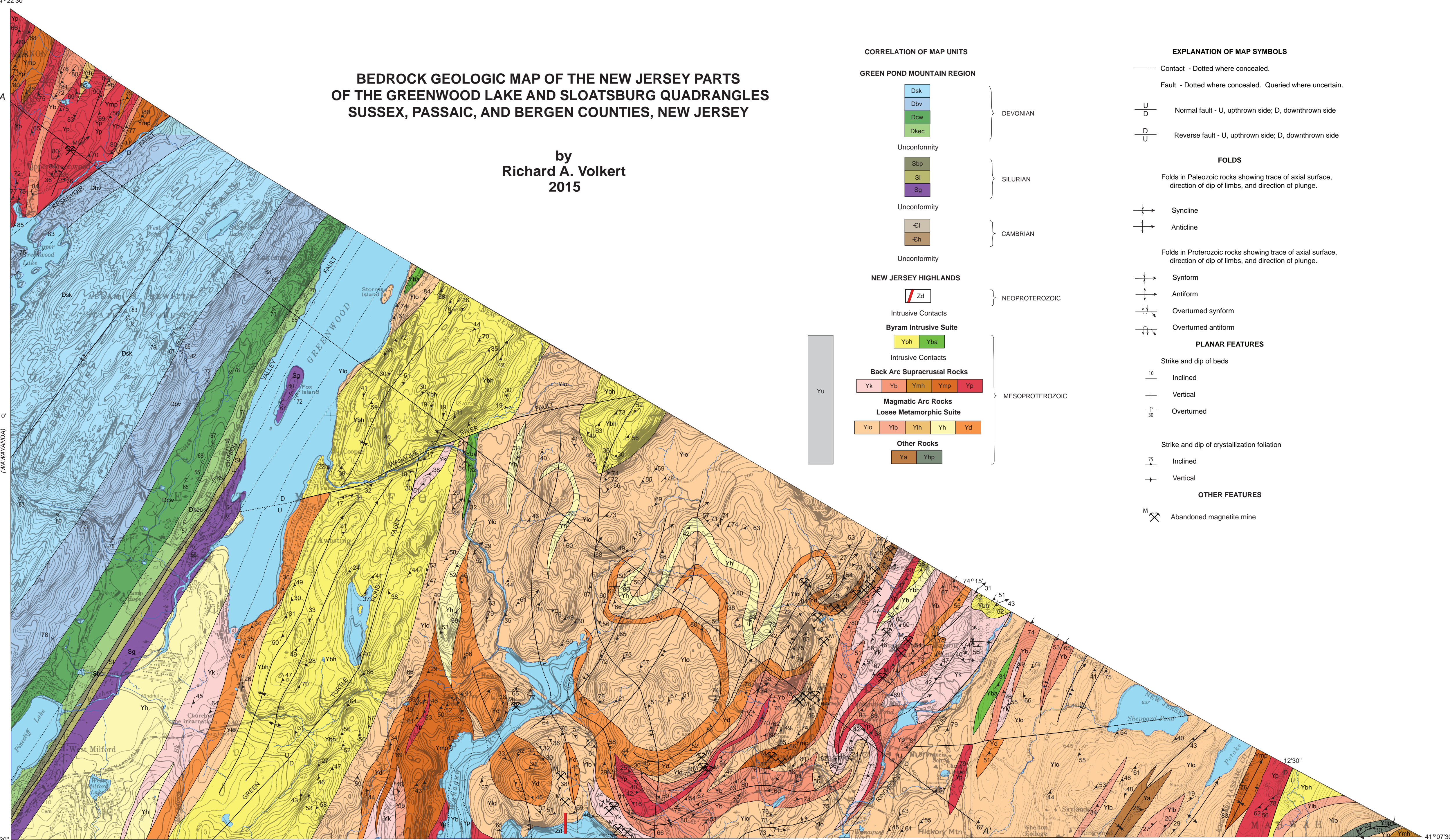


Figure 2. Rose diagram of the strike of crystallization foliations in Mesoproterozoic rocks of the Sloatsburg quadrangle.



Base maps from U.S. Geological Survey, 1954.
Bedrock geology mapped by R.A. Volkert in 1988, 2007, 2008
Paleozoic geology adopted from Herman and Mitchell (1991)
Digital cartography by M.W. Girard
Research supported by the U.S. Geological Survey, National Cooperative
Geological Mapping Program, under USGS award number 99HQAG0141
The views and conclusions contained in this document are those of the author
and should not be interpreted as necessarily representing the official
policies, either expressed or implied, of the U.S. Government.

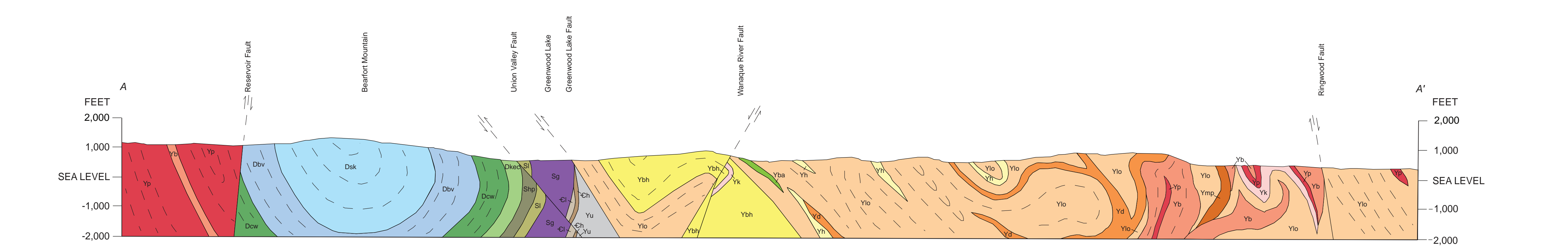
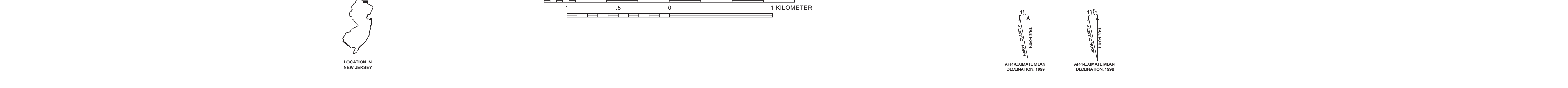


Figure 3. Rose diagram of the strike of joints in Mesoproterozoic rocks of the Greenwood Lake quadrangle.

Figure 4. Rose diagram of the strike of joints in Mesoproterozoic rocks of the Sloatsburg quadrangle.

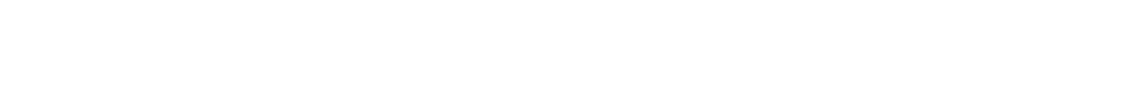


Figure 3. Rose diagram of the strike of joints in Mesoproterozoic rocks of the Greenwood Lake quadrangle.

Figure 4. Rose diagram of the strike of joints in Mesoproterozoic rocks of the Sloatsburg quadrangle.

Figure 5. Rose diagram of the strike of joints in Mesoproterozoic rocks of the Sloatsburg quadrangle.

Figure 6. Rose diagram of the strike of joints in Mesoproterozoic rocks of the Sloatsburg quadrangle.

Figure 7. Rose diagram of the strike of joints in Mesoproterozoic rocks of the Sloatsburg quadrangle.

Figure 8. Rose diagram of the strike of joints in Mesoproterozoic rocks of the Sloatsburg quadrangle.

Figure 9. Rose diagram of the strike of joints in Mesoproterozoic rocks of the Sloatsburg quadrangle.

Figure 10. Rose diagram of the strike of joints in Mesoproterozoic rocks of the Sloatsburg quadrangle.

Figure 11. Rose diagram of the strike of joints in Mesoproterozoic rocks of the Sloatsburg quadrangle.

Figure 12. Rose diagram of the strike of joints in Mesoproterozoic rocks of the Sloatsburg quadrangle.

Figure 13. Rose diagram of the strike of joints in Mesoproterozoic rocks of the Sloatsburg quadrangle.

Figure 14. Rose diagram of the strike of joints in Mesoproterozoic rocks of the Sloatsburg quadrangle.

Figure 15. Rose diagram of the strike of joints in Mesoproterozoic rocks of the Sloatsburg quadrangle.

Figure 16. Rose diagram of the strike of joints in Mesoproterozoic rocks of the Sloatsburg quadrangle.

Figure 17. Rose diagram of the strike of joints in Mesoproterozoic rocks of the Sloatsburg quadrangle.

Figure 18. Rose diagram of the strike of joints in Mesoproterozoic rocks of the Sloatsburg quadrangle.

Figure 19. Rose diagram of the strike of joints in Mesoproterozoic rocks of the Sloatsburg quadrangle.

Figure 20. Rose diagram of the strike of joints in Mesoproterozoic rocks of the Sloatsburg quadrangle.

Figure 21. Rose diagram of the strike of joints in Mesoproterozoic rocks of the Sloatsburg quadrangle.

Figure 22. Rose diagram of the strike of joints in Mesoproterozoic rocks of the Sloatsburg quadrangle.

Figure 23. Rose diagram of the strike of joints in Mesoproterozoic rocks of the Sloatsburg quadrangle.

Figure 24. Rose diagram of the strike of joints in Mesoproterozoic rocks of the Sloatsburg quadrangle.

Figure 25. Rose diagram of the strike of joints in Mesoproterozoic rocks of the Sloatsburg quadrangle.

Figure 26. Rose diagram of the strike of joints in Mesoproterozoic rocks of the Sloatsburg quadrangle.

Figure 27. Rose diagram of the strike of joints in Mesoproterozoic rocks of the Sloatsburg quadrangle.

Figure 28. Rose diagram of the strike of joints in Mesoproterozoic rocks of the Sloatsburg quadrangle.

Figure 29. Rose diagram of the strike of joints in Mesoproterozoic rocks of the Sloatsburg quadrangle.

Figure 30. Rose diagram of the strike of joints in Mesoproterozoic rocks of the Sloatsburg quadrangle.

Figure 31. Rose diagram of the strike of joints in Mesoproterozoic rocks of the Sloatsburg quadrangle.

Figure 32. Rose diagram of the strike of joints in Mesoproterozoic rocks of the Sloatsburg quadrangle.

Figure 33. Rose diagram of the strike of joints in Mesoproterozoic rocks of the Sloatsburg quadrangle.

Figure 34. Rose diagram of the strike of joints in Mesoproterozoic rocks of the Sloatsburg quadrangle.

Figure 35. Rose diagram of the strike of joints in Mesoproterozoic rocks of the Sloatsburg quadrangle.

Figure 36. Rose diagram of the strike of joints in Mesoproterozoic rocks of the Sloatsburg quadrangle.

Figure 37. Rose diagram of the strike of joints in Mesoproterozoic rocks of the Sloatsburg quadrangle.

Figure 38. Rose diagram of the strike of joints in Mesoproterozoic rocks of the Sloatsburg quadrangle.

Figure 39. Rose diagram of the strike of joints in Mesoproterozoic rocks of the Sloatsburg quadrangle.

Figure 40. Rose diagram of the strike of joints in Mesoproterozoic rocks of the Sloatsburg quadrangle.

Figure 41. Rose diagram of the strike of joints in Mesoproterozoic rocks of the Sloatsburg quadrangle.

Figure 42. Rose diagram of the strike of joints in Mesoproterozoic rocks of the Sloatsburg quadrangle.

Figure 43. Rose diagram of the strike of joints in Mesoproterozoic rocks of the Sloatsburg quadrangle.

Figure 44. Rose diagram of the strike of joints in Mesoproterozoic rocks of the Sloatsburg quadrangle.

Figure 45. Rose diagram of the strike of joints in Mesoproterozoic rocks of the Sloatsburg quadrangle.

Figure 46. Rose diagram of the strike of joints in Mesoproterozoic rocks of the Sloatsburg quadrangle.

Figure 47. Rose diagram of the strike of joints in Mesoproterozoic rocks of the Sloatsburg quadrangle.

Figure 48. Rose diagram of the strike of joints in Mesoproterozoic rocks of the Sloatsburg quadrangle.

Figure 49. Rose diagram of the strike of joints in Mesoproterozoic rocks of the Sloatsburg quadrangle.

Figure 50. Rose diagram of the strike of joints in Mesoproterozoic rocks of the Sloatsburg quadrangle.

Figure 51. Rose diagram of the strike of joints in Mesoproterozoic rocks of the Sloatsburg quadrangle.

Figure 52. Rose diagram of the strike of joints in Mesoproterozoic rocks of the Sloatsburg quadrangle.

Figure 53. Rose diagram of the strike of joints in Mesoproterozoic rocks of the Sloatsburg quadrangle.

Figure 54. Rose diagram of the strike of joints in Mesoproterozoic rocks of the Sloatsburg quadrangle.

Figure 55. Rose diagram of the strike of joints in Mesoproterozoic rocks of the Sloatsburg quadrangle.

Figure 56. Rose diagram of the strike of joints in Mesoproterozoic rocks of the Sloatsburg quadrangle.

Figure 57. Rose diagram of the strike of joints in Mesoproterozoic rocks of the Sloatsburg quadrangle.

Figure 58. Rose diagram of the strike of joints in Mesoproterozoic rocks of the Sloatsburg quadrangle.

Figure 59. Rose diagram of the strike of joints in Mesoproterozoic rocks of the Sloatsburg quadrangle.

Figure 60. Rose diagram of the strike of joints in Mesoproterozoic rocks of the Sloatsburg quadrangle.

Figure 61. Rose diagram of the strike of joints in Mesoproterozoic rocks of the Sloatsburg quadrangle.

Figure 62. Rose diagram of the strike of joints in Mesoproterozoic rocks of the Sloatsburg quadrangle.

Figure 63. Rose diagram of the strike of joints in Mesoproterozoic rocks of the Sloatsburg quadrangle.

Figure 64. Rose diagram of the strike of joints in Mesoproterozoic rocks of the Sloatsburg quadrangle.

Figure 65. Rose diagram of the strike of joints in Mesoproterozoic rocks of the Sloatsburg quadrangle.

Figure 66. Rose diagram of the strike of joints in Mesoproterozoic rocks of the Sloatsburg quadrangle.

Figure 67. Rose diagram of the strike of joints in Mesoproterozoic rocks of the Sloatsburg quadrangle.

Figure 68. Rose diagram of the strike of joints in Mesoproterozoic rocks of the Sloatsburg quadrangle.

Figure 69. Rose diagram of the strike of joints in Mesoproterozoic rocks of the Sloatsburg quadrangle.

Figure 70. Rose diagram of the strike of joints in Mesoproterozoic rocks of the Sloatsburg quadrangle.

Figure 71. Rose diagram of the strike of joints in Mesoproterozoic rocks of the Sloatsburg quadrangle.

Figure 72. Rose diagram of the strike of joints in Mesoproterozoic rocks of the Sloatsburg quadrangle.

Figure 73. Rose diagram of the strike of joints in Mesoproterozoic rocks of the Sloatsburg quadrangle.

Figure 74. Rose diagram of the strike of joints in Mesoproterozoic rocks of the Sloatsburg quadrangle.

Figure 75. Rose diagram of the strike of joints in Mesoproterozoic rocks of the Sloatsburg quadrangle.

Figure 76. Rose diagram of the strike of joints in Mesoproterozoic rocks of the Sloatsburg quadrangle.

Figure 77. Rose diagram of the strike of joints in Mesoproterozoic rocks of the Sloatsburg quadrangle.

Figure 78. Rose diagram of the strike of joints in Mesoproterozoic rocks of the Sloatsburg quadrangle.

Figure 79. Rose diagram of the strike of joints in Mesoproterozoic rocks of the Sloatsburg quadrangle.

Figure 80. Rose diagram of the strike of joints in Mesoproterozoic rocks of the Sloatsburg quadrangle.

Figure 81. Rose diagram of the strike of joints in Mesoproterozoic rocks of the Sloatsburg quadrangle.

Figure 82. Rose diagram of the strike of joints in Mesoproterozoic rocks of the Sloatsburg quadrangle.

Figure 83. Rose diagram of the strike of joints in Mesoproterozoic rocks of the Sloatsburg quadrangle.

Figure 84. Rose diagram of the strike of joints in Mesoproterozoic rocks of the Sloatsburg quadrangle.

Figure 85. Rose diagram of the strike of joints in Mesoproterozoic rocks of the Sloatsburg quadrangle.

Figure 86. Rose diagram of the strike of joints in Mesoproterozoic rocks of the Sloatsburg quadrangle.

Figure 87. Rose diagram of the strike of joints in Mesoproterozoic rocks of the Sloatsburg quadrangle.

Figure 88. Rose diagram of the strike of joints in Mesoproterozoic rocks of the Sloatsburg quadrangle.

Figure 89. Rose diagram of the strike of joints in Mesoproterozoic rocks of the Sloatsburg quadrangle.

Figure 90. Rose diagram of the strike of joints in Mesoproterozoic rocks of the Sloatsburg quadrangle.

Figure 91. Rose diagram of the strike of joints in Mesoproterozoic rocks of the Sloatsburg quadrangle.

Figure 92. Rose diagram of the strike of joints in Mesoproterozoic rocks of the Sloatsburg quadrangle.

Figure 93. Rose diagram of the strike of joints in Mesoproterozoic rocks of the Sloatsburg quadrangle.

Figure 94. Rose diagram of the strike of joints in Mesoproterozoic rocks of the Sloatsburg quadrangle.

Figure 95. Rose diagram of the strike of joints in Mesoproterozoic rocks of the Sloatsburg quadrangle.

Figure 96. Rose diagram of the strike of joints in Mesoproterozoic rocks of the Sloatsburg quadrangle.

Figure 97. Rose diagram of the strike of joints in Mesoproterozoic rocks of the Sloatsburg quadrangle.

Figure 98. Rose diagram of the strike of joints in Mesoproterozoic rocks of the Sloatsburg quadrangle.

Figure 99. Rose diagram of the strike of joints in Mesoproterozoic rocks of the Sloatsburg quadrangle.

Figure 100. Rose diagram of the strike of joints in Mesoproterozoic rocks of the Sloatsburg quadrangle.